LBL-27473
UC-404

Lawrence Berkeley Laboratory
UNIVERSITY OF CALIFORNIA

Materials & Chemical Sciences Division

Enhancement of Mass Transfer to a Rotating Cylinder Electrode by Inert Particles Suspended in the Electrolyte

L.H. Kim, R.H. Muller, and C.W. Tobias

June 1989

For Reference

Not to be taken from this room

LBL-27473
Copy 1
Bldg. 50 Library.

Prepared for the U.S. Department of Energy under Contract Number DE-AC03-76SF00098.

DISCLAIMER

This document was prepared as an account of work sponsored by the United States Government. While this document is believed to contain correct information, neither the United States Government nor any agency thereof, nor the Regents of the University of California, nor any of their employees, makes any warranty, express or implied, or assumes any legal responsibility for the accuracy, completeness, or usefulness of any information, apparatus, product, or process disclosed, or represents that its use would not infringe privately owned rights. Reference herein to any specific commercial product, process, or service by its trade name, trademark, manufacturer, or otherwise, does not necessarily constitute or imply its endorsement, recommendation, or favoring by the United States Government or any agency thereof, or the Regents of the University of California. The views and opinions of authors expressed herein do not necessarily state or reflect those of the United States Government or any agency thereof or the Regents of the University of California.

LBL-27473

ENHANCEMENT OF MASS TRANSFER TO A ROTATING CYLINDER ELECTRODE BY INERT PARTICLES SUSPENDED IN THE ELECTROLYTE

L. H. Kim, R. H. Muller, and C. W. Tobias*

Department of Chemical Engineering
and
Lawrence Berkeley Laboratory
University of California
Berkeley, California 94720

*Permanent address: Department of Chemical Engineering
Seoul National Polytechnic University
172 Gongnungdong Nowongu
Seoul, Republic of Korea

June 1989

ABSTRACT

Mass-transfer rates were investigated to a rotating cylindrical electrode in the presence of suspended particles either more or less dense than the electrolyte. In the case of low-density particles, the limiting-current density for the reduction of ferricyanide increases rapidly with volume fraction of solids up to about 10%, then gradually declines to values near those for the particle-free electrolyte. The transport process is interpreted by a three-zone model in which mass-transfer rate is controlled by different modes of particle behavior in the centrifugal force field. For high-density particles, limiting currents increase monotonically with increasing particle concentration, and the enhancement caused by suspended particles decreases with increasing rotation speed.

INTRODUCTION

Many electrochemical processes are limited by mass transport between a moving fluid and an electrode surface in contact with the fluid. To achieve high current densities, the thickness of the boundary layer has to be reduced. In this study, inert small particles suspended in the electrolyte are used for this purpose.

The mechanism of turbulent transport can be profoundly altered by the addition of inert small particles to the electrolyte (Ho and Leal, 1974). The rates of heat and mass transfer are significantly affected by suspended particles (Chung and Leal, 1982; Wang and Keller, 1985; Andersen et al., 1989), but the transport mechanism is poorly understood because of complicated phenomena between the wall and the suspension fluid.

Postlethwaite and Holdner (1975) attribute the enhancement of mass-transfer rates to the disruption of the boundary layer by the penetration of solid particles. These particles cause a diminution in the boundary-layer thickness, and they allow fresh liquid to be drawn into the diffusion layer because they carry their own film boundary layer. Smith and King (1975) also attribute the increase in the limiting-current density to an increased turbulence at the boundary layer due to the impingement of particles. Pini and Deanna (1977) qualitatively explained that the mass-transfer rate is determined by the thickness of the hydrodynamic boundary layer. With media containing solids, the laminar layer is changed locally by the impact of particles, or a local turbulence is set up with an intensity that depends on the number of impinging particles and their kinetic energy, leading to a local increase in the mass-transfer rate.

Roha (1981) investigated the effects of suspended glass beads (4–75 μm in diameter) on the rate of ferricyanide reduction at a rotating-disk electrode (RDE). The limiting current increased to more than three times its value without solids. This increase was greater at

high rotation speeds and with the larger disk electrodes. Ficquelment-Loizon et al. (1988) studied the influence of suspended particles on mass transfer to an RDE. They showed that mass flux can be increased or decreased by particles, and that the slope of the log I versus log Ω plot does not vary monotonically and can be lower than 0.5. They explain that these phenomena took place at the mass-exchange area and within the diffusion layer, their relative weights being changed by the variation in rotation speed. Andersen et al. (1989) studied the enhancement of limiting currents by suspended glass or polymer particles of various sizes (1–100 μm), using an RDE. Solid particles smaller than the thickness of the mass-transfer boundary layer create small-scale microconvective vortices. Particles much larger than the boundary-layer thickness appear to enhance transport by a different mechanism, possibly involving the formation of a particle-free wall layer.

The RDE has enjoyed wide popularity in electrochemical research, because its flow regime is stable over a wide range of rotation speeds and a uniform diffusion layer is established that can be computed accurately via the Levich theory. Most of the research described above was carried out using an RDE. However, the hydrodynamics in the radial direction are not uniform for large electrodes. By comparison, an advantage of the RCE over the RDE is that the current density and mass flux are uniform over the entire electrode surface. But the hydrodynamics of the RCE are almost always turbulent under practical operating conditions and consequently not accurately known.

In this report, we will discuss how mass-transfer rates are affected by inert solid spherical particles suspended in the flow of the RCE. The parameters are inherent in the hydrodynamics of the rotating cylinder, the particles, and the suspended medium. In particular, when non-neutrally buoyant particles are suspended at higher rotation speeds where the centrifugal force can dominate the movement of suspended particles, these particles move radially to the electrode surface. In this case, the resulting concentrated suspension may be expected to produce unusual effects on the mass-transfer rate.

MASS TRANSFER IN SUSPENSION FLUIDS

For turbulent flow generated entirely by an RCE, the hydrodynamics of the RCE are not accurately known. Thus, the mass-transfer-limited current at the RCE must be determined empirically. The dependence of the Sherwood (Sh) number on the hydrodynamic conditions and the relevant physical properties can be expressed in terms of the Reynolds (Re) and Schmidt (Sc) numbers:

$$Sh = a\, Re^{b}\, Sc^{c} \quad . \tag{1}$$

For the limiting-current condition,

$$K\, d_i/D = I_L\, d_i / z\, A\, F\, D\, C_b = a\, (U\, d_i / \nu)^{b}\, (\nu / D)^{c} \ , \tag{2}$$

or

$$I_L = a\, z\, A\, F\, C_b\, U^{b}\, d_i\, \nu^{c-b}\, D^{1-c} \ , \tag{3}$$

where z is the valence of the ion, F is the Faraday constant, A is the electrode area, C_b is the bulk concentration of species, d_i is the cylinder diameter, ν is the kinematic viscosity, D is the diffusion coefficient of the ferricyanide ion, and U is the peripheral velocity of the cylinder in cm/sec. A mass-transfer correlation was first proposed by Eisenberg, Tobias, and Wilke (1954) ($a = 0.0791$, $b = 0.7$, $c = 0.356$). Subsequent investigators confirmed the validity of this correlation, and their results have been reviewed by Gabe (1974) and Gabe and Walsh (1983).

For suspension fluids, the bulk diffusivity goes down, the viscosity increases, and the concentration of reacting species is diluted by particles. These changes in physical properties should decrease the limiting current. However, when inert particles are suspended in the solution, the limiting current increases in convective systems (Muller et

al., 1982; Wang and Keller, 1985; Andersen et al., 1989). This fact indicates that mass-transfer rates in suspension fluids cannot be predicted by what is known of the bulk behavior of suspension and the bulk properties. The hydrodynamic behavior of particles at the interface must be considered to interpret the transport process in suspension.

Variables affecting the behavior of the flowing suspension are (a) the motion of the individual particles, (b) the resultant radial variation of particle concentration, and (c) the velocity profiles for the suspending medium and suspended particles. The behavior is also affected by the properties of particles, such as size, shape, concentration, density, and sedimentation. Other factors include fluid inertia, centrifugal force, and non-Newtonian behavior of the suspension fluid. By assuming that the suspension fluid acts as a continuous medium in the RCE system, the limiting current can be written from equation (3) as :

$$I_L^* = a\, z\, A\, F\, C_b^*\, U^b\, d_i^{b-1}\, (\nu^*)^{c-b}\, (D^*)^{1-c} \qquad (4)$$

at the same geometry and the same rpm used in equation (3). We can derive the following equation from equations (3) and (4) :

$$I_L^*/I_L = f_1(\Phi)^{c-b}\, f_2(\Phi)^{1-c}\, f_3(\Phi = f(\Phi)\ , \qquad (5)$$

or

$$K^*/K = f_1(\Phi)^{c-b}\, f_2(\Phi)^{1-c}\ , \qquad (6)$$

where $\nu^*/\nu = f_1(\Phi)$, $D^*/D = f_2(\Phi)$, and $C_b^*/C_b = f_3(\Phi)$. If we apply the following empirical equations to the above equation for suspension fluids :

$$f_1(\Phi) = [1 + 2.5\Phi + 10.05\Phi^2 + 0.00273 \exp(16.6\Phi)]/[1+(\rho_s/\rho_f-1)\Phi] \text{ (Thomas, 1965)}, \qquad (7)$$

$$f_2(\Phi) = [8(2-\Phi)(1-\Phi)]/[(4+\Phi)(4-\Phi)] \text{ (Meredith and Tobias, 1963) } , \quad (8)$$

$$f_3(\Phi) = 1 - \Phi \quad , \quad (9)$$

$a = 0.0791$, $b = 0.7$, $c = 0.356$ (Eisenberg et al., 1954) ,

where the properties of the suspensions depend on the volume fraction Φ of suspended particles. Thus, I_L^*/I_L is derived only as the function of the volume fraction Φ :

$$I_L^*/I_L = f_1(\Phi)^{-0.344} f_2(\Phi)^{0.644} (1-\Phi) \quad , \quad (10)$$

$$[K^*/K = f_1(\Phi)^{-0.344} f_2(\Phi)^{0.644} \quad . \quad (11)$$

EXPERIMENTAL

The RCE and cell

The rotating concentric cylinder cell used in our experiments and a schematic view of the RCE assembly are shown in Fig. 1. The essential elements of the cell are a stationary outer cylinder made of PTFE, in which a nickel anode is embedded, and an inner rotating cylinder on which the cathode is mounted in insulating PTFE, leaving exposed only the platinum electrode surface 8.5 mm above the bottom of the cell. The anode is 25.4 mm high, and the inner diameter of the cell is 25.4 mm. The cathode is 25.4 mm high, and the outer diameter is 8.5 mm. Thus the annular gap formed by the cylinder is 8.5 mm. The cathode is situated at the same height as the anode to ensure a uniform current distribution.

The cathode was connected to the potentiostat through a stainless steel rod inside the inner PTFE cylinder. The cylinder was driven by a stabilized dc motor and controlled to within 1.0% of a selected speed by a Pine Model ASR-2 rotator (Pine Instrument Co., Grove City, PA). The cylinder rotation speeds varied from 1000 to 6000 rpm, equivalent to a peripheral velocity of 44.35 to 266.09 cm sec^{-1}. The bulk flow patterns corresponding to

these rpm ranges were completely turbulent flows. Before taking a series of measurements, the electrode was washed with detergent, distilled water, and acetone, and then subjected to cathodic activation in the same electrolyte.

Electrical circuit

The electrical circuit is shown in Fig. 2. Current was supplied to the cell by a PARC Model 173 potentiostat (Princeton Applied Research, Princeton, NJ). A PARC Model 175 universal programmer was used to ramp or step the applied potential; the potential of the working electrode was monitored with a high-impedance digital voltmeter (model 173A, Keithley, Cleveland, OH), using a potential pick-up brush located near the working electrode. Currents and voltages were plotted on an X-Y recorder (Model 7044B, Hewlett-Packard Co., Palo Alto, CA) and stored in a data-acquisition system (IBM PS/2, Model 50Z).

Electrolyte

The electrolyte used was an aqueous solution of 2.0M NaOH supporting a mixture of 0.04M $K_3Fe(CN)_6$ and 0.2M $K_4Fe(CN)_6 \cdot 3H_2O$. The latter concentration was chosen to have diffusional limitation at the cathode only. The large excess of the NaOH supporting electrolyte caused ionic migration in the potential gradient to be negligibly small. The solution was stored in the dark. The bulk concentrations were determined and checked by titration. The required amounts of salts were weighed, and the true ferricyanide concentration was determined by a back titration of iodine with $Na_2S_2O_3$.

The diffusion coefficient D of the ferricyanide ion in the solution was calculated from the literature (Gordon et al., 1966). The kinematic viscosity ν and the density of the electrolyte solution were also taken from the literature (Boeffard, 1966). The calculated values were

$D = 4.50 \times 10^{-5}$ cm^2 sec^{-1}, and $\nu = 1.372 \times 10^{-2}$ cm^2 sec^{-1}. The electrolyte composition was kept constant. The solution temperature was set at 22 ± 0.5°C.

Particles

The experiments in this study were carried out using soda-lime glass beads (density = 2.48 g/cm^3), previously obtained by Roha (1981) and Andersen et al. (1989) from Potters Industries, and hollow glass beads (density = 0.305 g/cm^3), with a low density relative to the electrolyte. A scanning electron micrograph (Fig. 3) shows that most of the hollow glass beads were nearly spherical. The particles were classified using standard Tyler sieves. Particle sizes were determined from measurements of micrographs and a volume-weighed average diameter. The glass beads are called high-density or low-density particles, depending on their density relative to that of the electrolyte.

RESULTS AND DISCUSSION

Experiments were repeated several times with good reproducibility. The experimental data were obtained at rotation speeds higher than 1000 rpm to minimize buoyancy and sedimentation effects.

Limiting-current measurement

The limiting-current technique is often used in mass-transfer investigations in electrochemical systems. Problems arise with this technique when the surface area of the electrode changes due to rapid etching or rough cathodic electrodeposition; when steady-state limiting currents are established slowly; or when the solution concentration falls rapidly due to depletion in the small-volume reactor. To avoid these problems in the present study, reduction of ferricyanide was selected as the electrode reaction, and the potential-step technique for determining limiting-current densities was used under turbulent-flow conditions. The determination of a limiting overpotential E_L, which

corresponds to the limiting-current condition, has been described in several reviews (Selman and Tobias, 1978; Gabe and Makanjuola, 1986). The value of E_L has been established in a preliminary potentiodynamic sweep. E_L was subsequently used in a potentiostatic measurement in which I was plotted against time, and I_L was the steady value. The value of E_L was -500 ± 10 mV in the electrolyte without suspended particles. This potential, corresponding to the limiting diffusion plateau, was imposed at the working electrode. During each run a potential step was applied for 90 sec after the desired rotational speed had been reached.

Mass transfer without particles

Limiting currents were measured in the RCE system for the electrolyte medium without particles. The experimental Sherwood numbers were obtained from the measured limiting currents by equation (1). The Sherwood-number versus Reynolds-number plot exhibits a straight line of slope 0.67, as shown in Fig. 4. Literature data for the exponent of the Reynolds number range from 0.6 to 0.7 (Matic et al., 1978; Eisenberg et al., 1955). The dashed line represents the values calculated by the correlation of Eisenberg et al. (1954) (ETW correlation). Experimental mass-transfer rates were within 3% of values calculated by the ETW correlation for our experimental range ($689 < Re < 16539$, $Sc = 3048$).

Limiting currents with low-density glass particles

When low-density particles were added to the electrolyte medium, limiting currents were measured over 1–40% particle volume fractions and rotation speeds of the inner cylinder of 1000 to 5000 rpm. Limiting currents I_L* are plotted against the particle concentration Φ in Fig. 5. As Φ increased, the limiting currents increased up to a particle concentration corresponding to a maximum limiting-current density. Specifically, limiting currents were significantly enhanced by the particles at dilute volume fraction. As shown in Fig. 5, I_L* was higher than the limiting current for the electrolyte without particles by a factor of 2, and

then decreased at higher particle concentrations. It appears that there is an optimal value of particle concentration that leads to a maximum limiting-current density at a given rotation speed. Earlier investigations have established that, for a given rotation speed and particle concentration, an optimal value of particle size leads to a maximum in the mass-flux increase (Roha, 1981). Similarly, a threshold particle concentration of about 7–10% was reported as necessary to promote mass transfer (Roha, 1981). At low (< 2000) rpm, this decrease in limiting current varies monotonically in our experimental range (up to 40 vol%). However, at higher (> 2500) rpm, limiting currents are constant only at the higher particle concentrations (> 30 vol%). The ratio of mass-transfer coefficient K*/K was plotted against particle concentration. As shown in Fig. 6, plots do not vary monotonically, and K*/K, which shows the influence of mass-transfer enhancement induced by the particles, is larger than the values calculated by equation (11). In the higher particle-concentration range ($\Phi > 0.2$), K*/K decreases with increasing rpm, as shown in Fig. 6.

A typical I_L* versus Φ curve is shown in Fig. 7. In the constant limiting-current range, oscillation of current values occurs in the current-potential curve. For dilute suspensions, the limiting current does not fluctuate in our experimental range (< 5000 rpm). However, at higher volume fractions and higher rotation speeds, the limiting current fluctuates more frequently and with a higher intensity. Three different controlling mechanisms of mass transfer may be identified on this curve by three regions. These regions are discussed below.

Region A. When the particles lower in density relative to the medium are added to the RCE system, there is inward migration of particles from the bulk suspension because of the centrifugal force. However, the motion of particles by orbital drift is outward from the inner rotating cylinder. In addition, the effect of collisions between particles tends to distribute the suspending fluid uniformly. Therefore, the particles would migrate to an

equilibrium position by a balance of the above-described forces (Ho and Leal, 1974), and would probably form an annular ring band with a higher than average particle concentration. In this case, we could postulate a particle-free diffusion layer between the electrode surface and the annular ring band (Andersen et al., 1989; Segré and Silverberg, 1962). The formation of this particle-free layer has been observed by other researchers (Mashelkar and Dutta, 1982; Watkins et al., 1976). As rotation speeds are increased in region A, the annular ring forms progressively closer to the electrode surface, so that the thickness of the particle-free layer is reduced and the slip by particles at the interface increases. On the other hand, the annular particle ring may be disturbed and expanded by an increase in turbulent intensity with increasing rpm. Each particle comes into less frequent contact with its neighbors and is consequently able to rotate more freely, even at higher particle concentrations, so that the influence of microconvective flow by the shear-induced rotation of particles is increased. Thus, as both rotation speed and particle concentration are increased, the limiting current increases in region A. The particle concentration at which a maximum limiting current appears increases. For example, in Fig. 5, at 1000 rpm the maximum limiting current corresponds to $\Phi = 1$ vol%, while at 5000 rpm, the maximum limiting current occurs at $\Phi = 10$ vol%.

Region B. As the particle concentration is increased at a given rotation speed, the annular particle ring becomes thicker so that the mass transfer of ions from the bulk is inhibited by this porous particle layer. In addition, the increase in local particle concentration leads to a hindrance in the free rotation of particles so that the influence of the mass-transfer enhancement due to the collision and shear-induced rotation of particles becomes smaller. These phenomena result in a decrease in mass transfer. Therefore, limiting currents would decrease with increasing particle concentration in region B. However, there may still be a particle-free layer between the electrode surface and the

annular particle ring. Mass transfer is controlled by the same hydrodynamic mechanism as in region A. This is confirmed indirectly by the experimental results shown in Fig. 7.

Region C. At still higher particle concentrations (about $\Phi > 0.3$), as the rotation speed is increased, a more compact particle layer may form at the interface, resulting in a structure similar to a porous medium. In the extreme, the particles concentrated closest to the inner electrode surface by centrifugal force can build up clumps or clusters. Depending on their size, the larger clusters may migrate to positions closer to the electrode surface than the smaller ones. Finally, the large clusters may adhere to the cathode surface. The clusters may increase to any size that can withstand the drag force. These clusters may interfere with ion transfer to the cathode and also reduce the active area of the electrode surface (Scheller et al., 1970; Caprani and Frayert, 1982; Caprani et al., 1988). When these clusters detach from the surface or break up, the limiting current will suddenly increase. These phenomena take place more frequently at high volume fractions and high rpm so that intense fluctuations of limiting current will occur.

Effect of rotation speed on limiting currents

To evaluate the influence of the hydrodynamics in the RCE on mass-transfer rates, log I_L* was plotted versus log rpm in Fig. 8. The plots are straight lines except at the 40 vol% particle concentration. The slopes of the curves are almost identical to the slopes without particles. Barkey (1987) measured limiting currents from a dense suspension of 80-μm glass spheres in an RCE system with baffles in place and with protruding sleeves on the electrode. His results were similar: limiting currents varied as the 0.7 power of the rotation rate. The values of limiting currents were higher by a factor of 1.3 than those for the electrolyte without spheres in the cell with baffles. For higher particle concentrations and higher rotation speeds (40 vol%, > 2500 rpm), the limiting currents did not increase with increasing rpm and reached constant values. Generally, mass-transfer rates increased

with higher particle concentration and higher rotation speed due to increase in turbulence intensity. This contradiction with our experimental results can be explained by the clump formation and the blocking effects, as described above.

Effect of particle size on limiting currents

Two different sizes of suspended particles were used to study the effect of particle size on limiting current. In the flow generated by the RDE, Andersen et al. (1989) showed that mass-transfer enhancement was controlled by a different transport mechanism, depending on the size of particles relative to the thickness of the boundary layer. Particles smaller than, or comparable to, the thickness of the boundary layer were more effective in enhancing mass transfer. To avoid this complication, all particles used in this work were larger than the boundary-layer thickness (calculated by ETW correlation). At a given particle concentration (10 vol%), limiting currents for the larger particles (68 μm) were higher than those for smaller particles (30 μm), as shown in Fig. 9. One likely explanation for this size effect may be migration of particles to the electrode surface; i.e., under the effect of centrifugal force, larger particles can move closer to the interface than smaller ones. Particles close to the electrode surface can disturb the mass-transfer boundary layer, thereby increasing the limiting currents.

Mass transfer in high-density glass-particle suspension

A plot of I_L^*/I_L vs concentration is shown in Fig. 10 for high-density glass beads (ρ_s/ρ_f = 2.19) . The value of I_L^*/I_L increased monotonically with increasing particle concentration and decreased with increasing rotation speed. All experimental limiting currents were larger than those calculated by equation (10). For increased particle concentration at a given rpm, the particle concentration in the boundary layer of the inner cylinder may be dilute even at the higher concentration, because the high-density particles migrated outward

in the centrifugal force field. Therefore, the transport mechanisms controlled would correspond to region A, and consequently, limiting currents would increase.

On the other hand, as the rpm increased at a given particle concentration, the number of particles able to disturb the inner electrode surface would decrease due to the increase in centrifugal force. In addition, microconvection by rotation and by particle-particle and particle-wall collisions may also increase due to the more intense turbulence. The former phenomenon will decrease the influence of particles on mass-transfer enhancement, while the latter phenomenon will increase it. The factor of enhancement by suspended particles I_L^*/I_L decreased with increasing rotation speed, as shown in Fig. 10. Based on the above discussion, the results show that the transport mechanisms in the high-density particle suspension are also controlled by the effects of centrifugal force.

CONCLUSIONS

Limiting currents at rotating-cylinder electrodes, measured in an electrolyte without particles, agreed well with those calculated by the ETW correlation. Limiting-current density varied with the 0.67 power versus rpm in our experimental range ($689 < Re < 16539$). On the other hand, when inert low-density particles ($\rho_s/\rho_f = 0.27$) were suspended in the electrolyte with the same cell geometry, mass-transfer rates were controlled by the centrifugal force in the same rpm range. Limiting currents also varied with almost the same power (slope = 0.7–0.67) versus rpm, except in the range showing the blocking effects. Specifically, limiting-current densities increased rapidly at dilute particle concentration. This high mass-transfer enhancement resulted from disturbance of the boundary layer by the particles concentrated at the electrode surface in the centrifugal force field. This result is important in industrial applications that require high mass-transfer rates, because, generally, the increase in particle concentration accompanies problems of reactor corrosion and higher power requirement. Transport phenomena were interpreted by a model with three different regimes of particle volume fractions. When high-density particles ($\rho_s/\rho_f = 2.19$) were suspended in the electrolyte, limiting currents increased monotonically with increased particle concentration. However, I_L^*/I_L decreased with increasing rotation speed, because high-density particles migrate outward in the centrifugal force field.

ACKNOWLEDGEMENT

This work was supported jointly by the Director, Office of Energy Research, Office of Basic Energy Sciences, Materials Sciences Division, of the U.S. Department of Energy under Contract No. DE-AC03-76SF00098; L.H. Kim was supported by the Korea Science and Engineering Foundation.

LIST OF SYMBOLS

a	constant, equation (1)
A	active area of the cathode, cm^2
b	exponent on Reynolds number
c	exponent on Schmidt number
C	concentration, moles/liter
d	cylinder diameter, cm or mm
D	diffusivity, cm^2/sec
E	overpotential, volts
f_1	dimensionless kinematic viscosity function, equation (7)
f_2	dimensionless diffusivity function, equation (8)
f_3	dimensionless concentration function, equation (9)
F	Faraday's constant, 96,487 Coulombs/equiv.
I	current density, mA/cm^2
K	mass-transfer coefficient, cm/sec
Re	Reynolds number
Sc	Schmidt number
Sh	Sherwood number
z	number of electrons in electrode reaction, equiv./mole

Greek Letters

μ	viscosity, g/cm-sec
ν	kinematic viscosity, cm^2/sec
Ω	rotation speed of the cylinder electrode, rpm
π	3.14159
ρ	density, g/cm^3
Φ	particle volume fraction (or volume percent) of suspended phase

Subscripts

b	bulk phase
i	inner cylinder
f	fluid phase
L	limiting value

s solid phase

Superscript

* suspension property

REFERENCES

1. P.K. Andersen, R.H. Muller, and C.W.Tobias, " The Effect of Suspended Solids on Mass Transfer to a Rotating Disk," *J. Electrochem. Soc.* 136, 390 (1989).

2. D.P.Barkey, "Studies on High Speed Electroforming," Ph.D. Thesis, University of California at Berkeley, LBL-23880 (1987).

3. A.J. Boeffard, "Ionic Mass Transfer by Free Convection in a Redox System," M.S. Thesis, University of California at Berkeley (1966).

4. A. Caprani and J.P.Frayert, "Interactions Between Oxygen Reduction and Titanium Dissolution in Aerated Hydrochloric Acid," *J. Electroanal. Chem.* 138, 155 (1982).

5. A. Caprani, M.M. de Ficquelmont-Loizos, L. Tamisier, and P. Peronneau, "Mass Transfer in Laminar Flow at a Rotating Disk Electrode in Suspensions of Inert Particles, Part 2; Theoretical Evaluation of Experimental Results," *J. Electrochem. Soc.* 135, 635 (1988).

6. Y.C. Chung and L.G. Leal, "An Experimental Study of the Effective Thermal Conductivity of a Sheared Suspension of Rigid Spheres," *Int. J. Multiphase Flow* 8, 605 (1982).

7. M. Eisenberg, C.W. Tobias, and C.R. Wilke, "Ionic Mass Transfer and Concentration Polarization at Rotating Electrodes," *J. Electrochem. Soc.* 101, 306 (1954).

8. M. Eisenberg, C.W. Tobias, and C. R. Wilke, "Mass Transfer at Rotating Cylinders," *Chem. Eng. Prog. Symp. Series* No. 16, 51 (1955).

9. M.M. de Ficquelmont-Loizos, L. Tamisier, and A. Caprani, "Mass Transfer in Laminar Flow at a Rotating Disk Electrode in Suspensions of Inert Particles, Part 1; Experimental Investigation on Influence of the Electrode, the Medium, and the Particles," *J. Electrochem. Soc.* 135, 626 (1988).

10. D.R. Gabe, "The Rotating Cylinder Electrode," *J. Appl. Electrochem.* 4, 91 (1974).

11. D. R. Gabe and P.A. Makanjuola, "Determination of Limiting Currents: A Potential-Step Technique," *IChemE Symp. Series* No. 98, 309 (1986).

12. D.R. Gabe and F.C. Walsh, "The Rotating Cylinder Electrode: a Review of Development," *J. Appl. Electrochem.* 13, 3 (1983).

13. S.L. Gordon, J.S. Newman, and C.W. Tobias, "The Role of Ionic Migration in Electrolytic Mass Transport; Diffusivities of $[Fe(CN)_6]^{3-}$ and $[Fe(CN)_6]^{4-}$ in KOH and NaOH Solutions," *Berichte der Bunsengesellschaft für physikalische Chemie* 70, 414 (1966).

14. B.P. Ho and L.G. Leal, "Inertia Migration of Rigid Spheres in Two-Dimensional Unidirectional Flows," *J. Fluid Mech.* 65, 365 (1974).

15. R.A. Mashelkar and A. Dutta, "Convective Diffusion in Structured Fluids: Need for New Analysis and Design Strategies," *Chem. Eng. Sci.* 37, 969 (1982).

16. D. Matic, B. Lovrecek, and D. Skansi, "The Rotating Cylinder Electrode," *J. Appl. Electrochem.* 8, 391 (1978).

17. R.E. Meredith and C.W. Tobias, "Resistance to Potential Flow though a Cubical Array of Spheres," *J. Appl. Phys.* 31, 1270 (1963).

18. R.H. Muller, D.J. Roha, and C.W. Tobias, "Effect of Suspended Particles on the Rate of Mass Transfer to a Rotating Disk Electrode," in *Transport Processes in Electrochemical System,* R.S. Yeo, T. Katan, and D.T Chin, Eds., p. 1; vol. 82–10 in The Electrochemical Society Softbound Proceedings Series, Pennington, NJ (1982).

19. G.C. Pini and P.L. Deanna, "Influence of Suspended Particles on Mass Transfer under Turbulent Conditions at a Rotated Disk Electrode," *Electrochimca Acta* 22, 1432 (1977).

20. J. Postlethwaite and D.N. Holdner, "Wall Mass Transfer in Horizontal Slurry Pipeline," *Can. J. Chem. Eng.* 53, 31 (1975).

21. D.J. Roha, "Effect of Suspended Particles on the Rate of Mass Transfer to a Rotating Disk Electrode," M.S. Thesis, University of California at Berkeley (1981).

22. G. Segre' and A. Silberberg, "Behavior of Microscopic Rigid Spheres in Poiseuille Flow. Part 2. Experimental Results and Interpretation," J. *Fluid Mech.* 14, 136 (1962).

23. F. Scheller, R. Landsberg, and H. Wolf, "Zur Bestimmung des Blockierungsgrades an Teilweise Blockierten Festelektroden," *Electrochimica Acta* 15, 525 (1970).

24. J.R. Selman and C.W. Tobias, "Mass-Transfer Measurement by the Limiting-Current Technique, " *Advances in Chemical Engineering* 10, 211 (1978).

25. J.W. Smith and D.H. King, "Electrochemical Wall Mass Transfer in Liquid Particulate System," *Can. J. Chem. Eng.* 53, 41 (1975).

26. D.G. Thomas, "Transport Characteristics of Suspensions: VIII. A Note on the Viscosity of Newtonian Suspensions of Uniform Spherical Particles," *J. Colloid Sci.* 20, 267 (1965).

27. N.L. Wang and K.H. Keller, "Augmented Transport of Extracellular Solutes in Concentrated Erythrocyte Suspensions in Couette Flow," *J. Colloid Interface Sci.* 103, 210 (1985).

28. R.W. Watkins, C.R. Robertson, and A. Acrivos, "Entrance Region Heat Transfer in Flowing Suspensions," *Int. J. Heat Mass Transfer* 19, 693 (1976).

FIGURE CAPTIONS

Figure 1. Rotating-cylinder electrode and electrochemical cell. The cathode diameter is 0.85 cm, and the active platinum electrode area of the cathode is 6.79 cm^2. (XBL 896-2420)

Figure 2. Schematic of electrical circuit. R, C, and W on the potentiostat refer to the reference electrode, counter electrode, and working electrode, respectively. (XBL 896-2421)

Figure 3. Scanning electron micrograph (×169) of the hollow glass particles, showing that their shape is nearly spherical. (XBB 896-5281)

Figure 4. Comparison between experimental results and values calculated by the ETW correlation in an electrolyte solution containing particles [0.04M $K_3Fe(CN)_6$ + 0.2M $K_4Fe(CN)_6 \cdot 3H_2O$ + 2M NaOH]. (XBL 896-2422)

Figure 5. Variation in limiting-current density I_L* with particle concentration Φ and rotation speed. The suspended particles are hollow glass beads (size range = 63 – 74 μm, average diameter = 68 μm, density = 0.305 g/cm^3, ρ_s/ρ_f = 0.27); electrolyte medium is 0.04M $K_3Fe(CN)_6$ + 0.2M $K_4Fe(CN)_6$ $3H_2O$ + 2M NaOH. (XBL 896-2423)

Figure 6. Variation of K_L*/K_L with particle concentration Φ at different rotation speeds, where K_L* is the mass-transfer coefficient from the particle-suspension electrolyte and K_L is the mass-transfer coefficient from the electrolyte without particles. Suspended particles are hollow glass beads (size range = 63 – 74 μm, average diameter = 68 μm, density = 0.305 g/cm^3, ρ_s/ρ_f = 0.27); electrolyte medium is 0.04 M $K_3Fe(CN)_6$ + 0.2M $K_4Fe(CN)_* 3H_2O$ + 2M NaOH. The theoretical values are calculated by equation (11). (XBL 896-2424)

Figure 7. Typical curve of limiting-current density versus particle concentration at a given rotation speed (4000 rpm). Error bars indicate the range of limiting-current fluctuations. (XBL 896-2425)

Figure 8. Limiting-current density (log I_L*) of suspensions with hollow glass beads as a function of rotation speed (log rpm) for different particle concentrations. The line represents a least-squares fit to the data. (XBL 896-2426)

Figure 9. Variation of limiting-current density with particle size and rotation speed at a given particle concentration (10 vol%), using particles of two different average diameters. (XBL 896-2427)

Figure 10. Variation of I_L^*/I_L versus particle concentration Φ with rotation speed, where I_L^* is the limiting-current density of the electrolyte with suspended particles and I_L is the limiting-current density of the electrolyte without particles. Suspended particles are high-density glass beads (size range = 63 – 106 μm, average diameter = 80 μm, density = 2.48 g/cm^3, $\rho_s/\rho_f = 2.19$); electrolyte medium is 0.04M $K_3Fe(CN)_6$ + 0.2M $K_4Fe(CN)_6 \cdot 3H_2O$ + 2M NaOH. The theoretical values are calculated by equation (10). (XBL 895-2428)

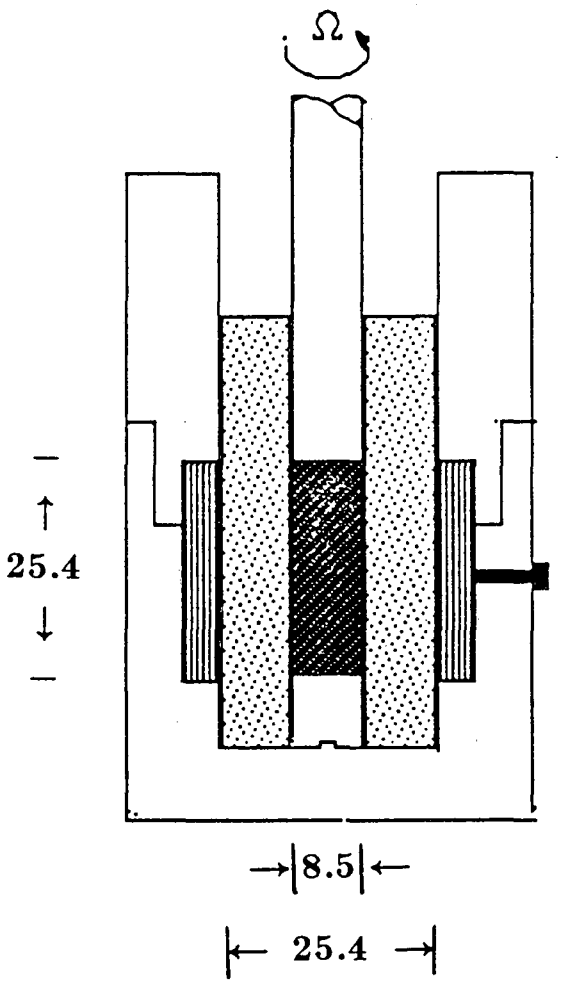

Cathode (platinum)
Anode (nickel)
Outer cylinder (PTFE)
Suspended electrolyte
[$K_3Fe(CN)_6 + K_4Fe(CN)_6 + NaOH$ + glass beads]
Units are mm

XBL 896-2420

Figure 1

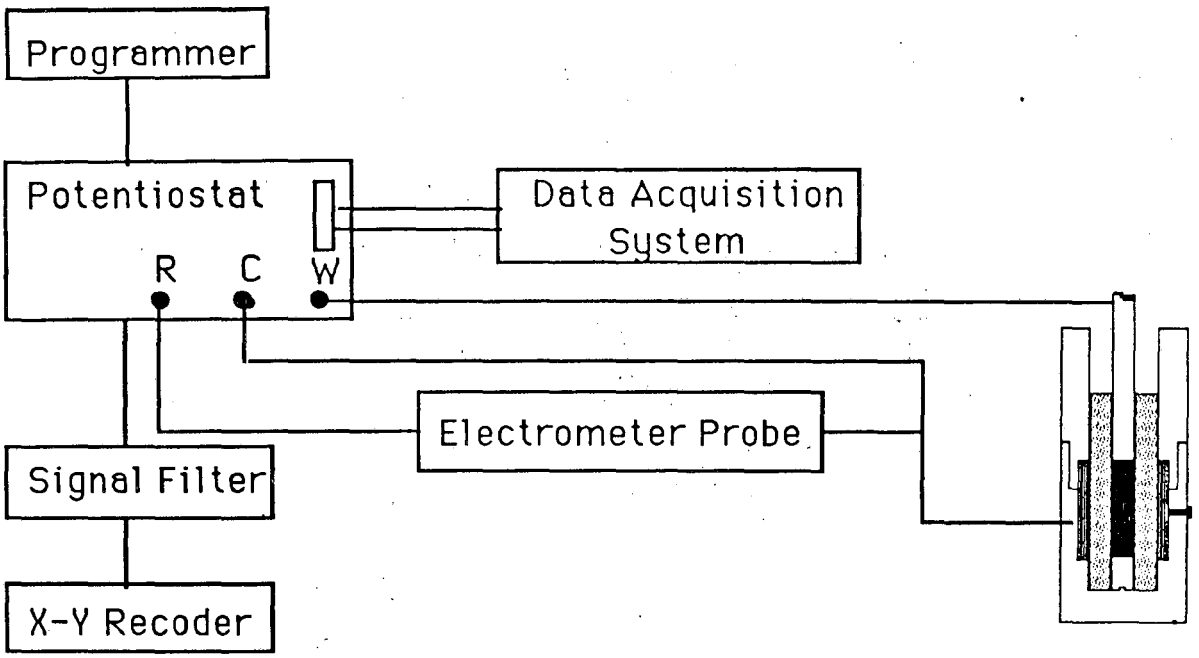

XBL 896-2421

Figure 2

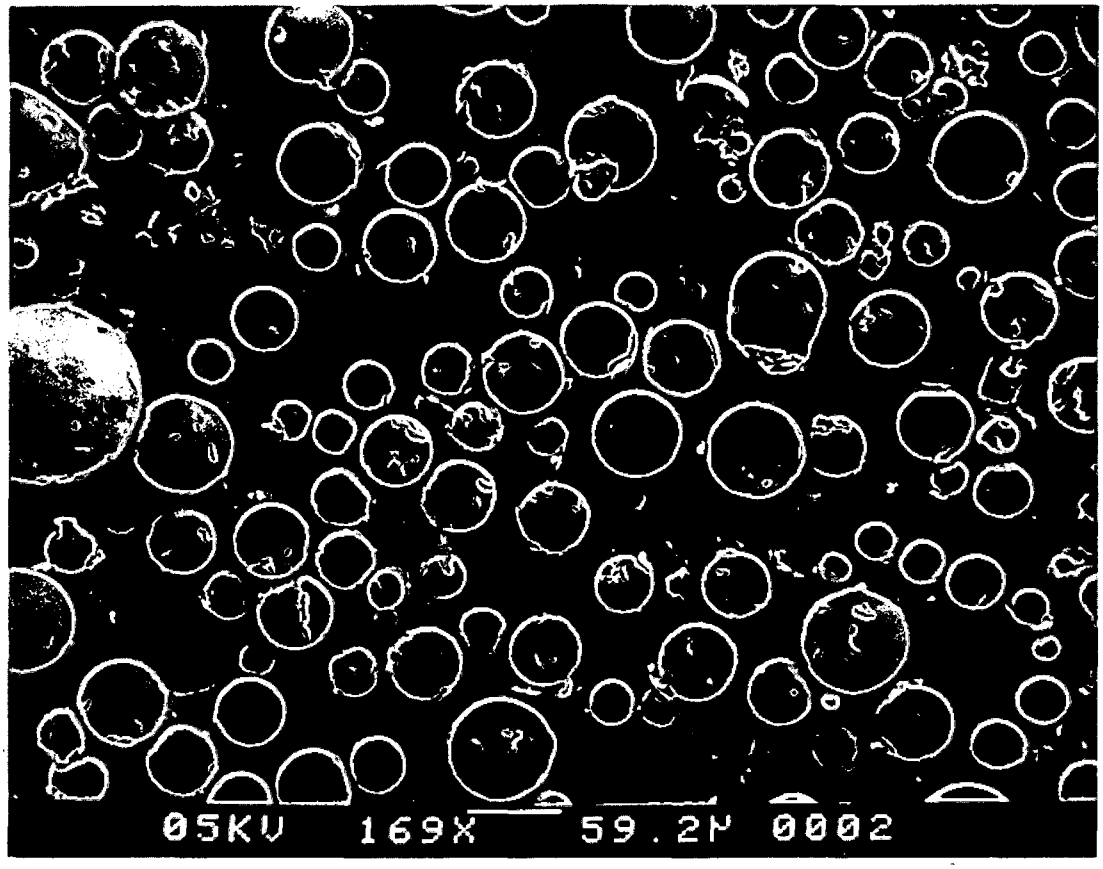

XBB 896-5281

Figure 3

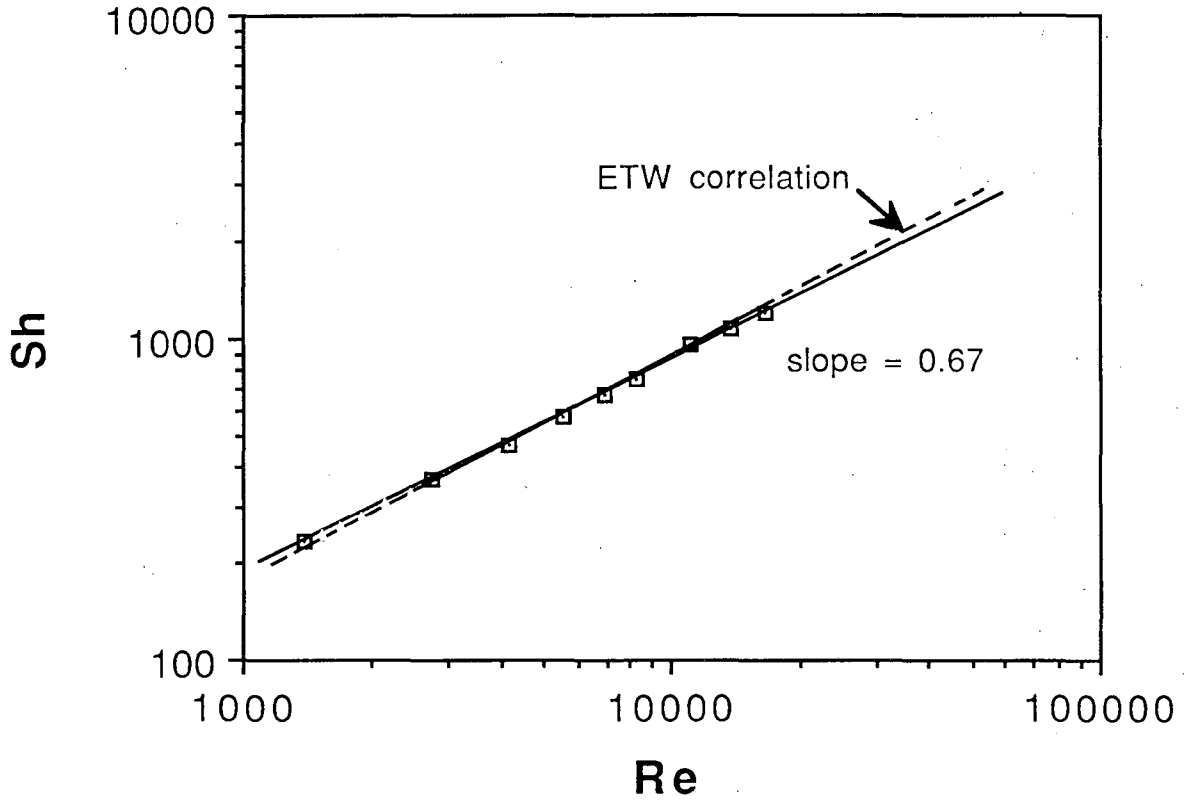

XBL 896-2422

Figure 4

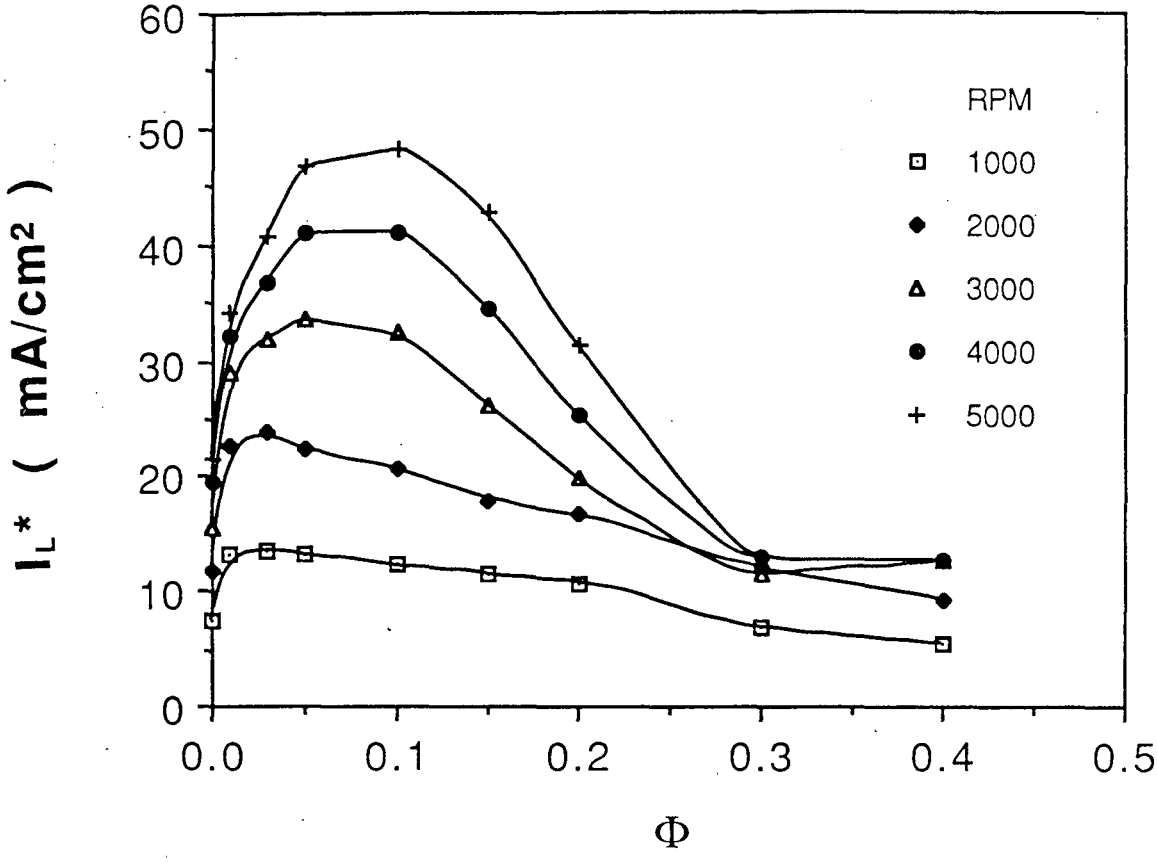

XBL 896-2423

Figure 5

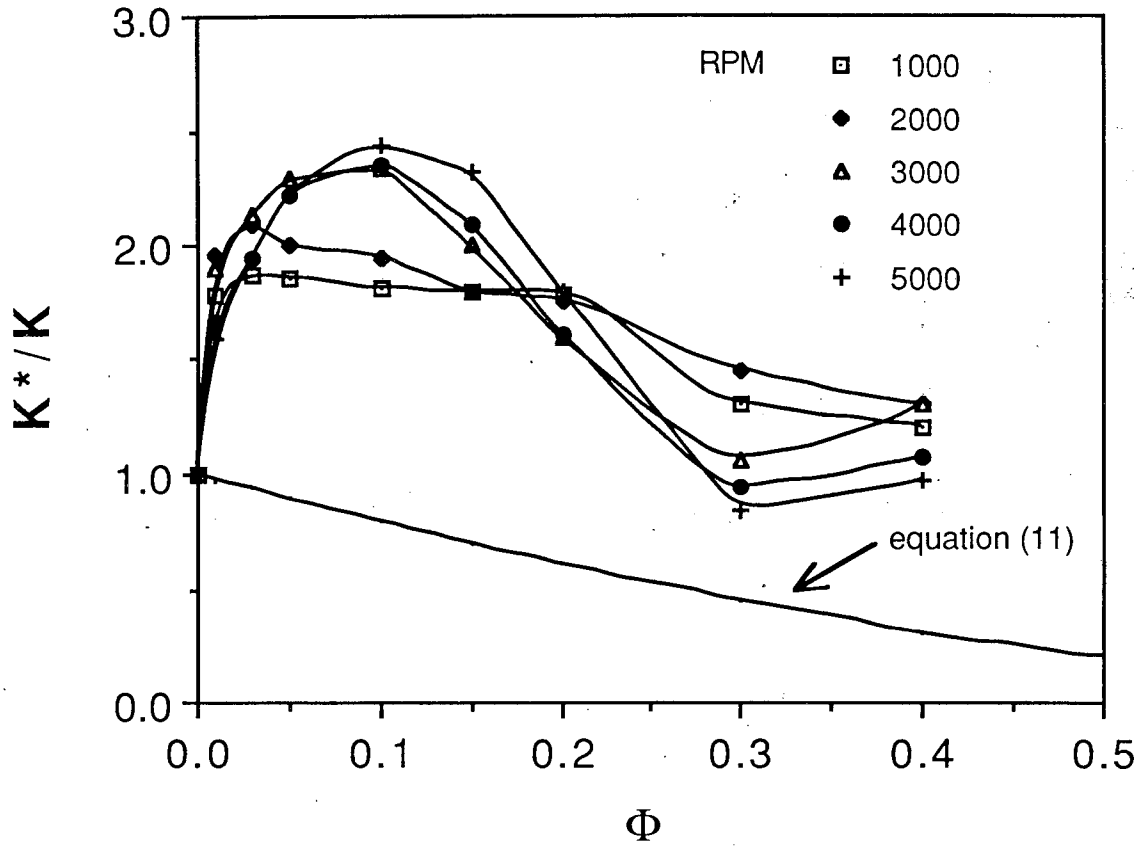

XBL 896-2424

Figure 6

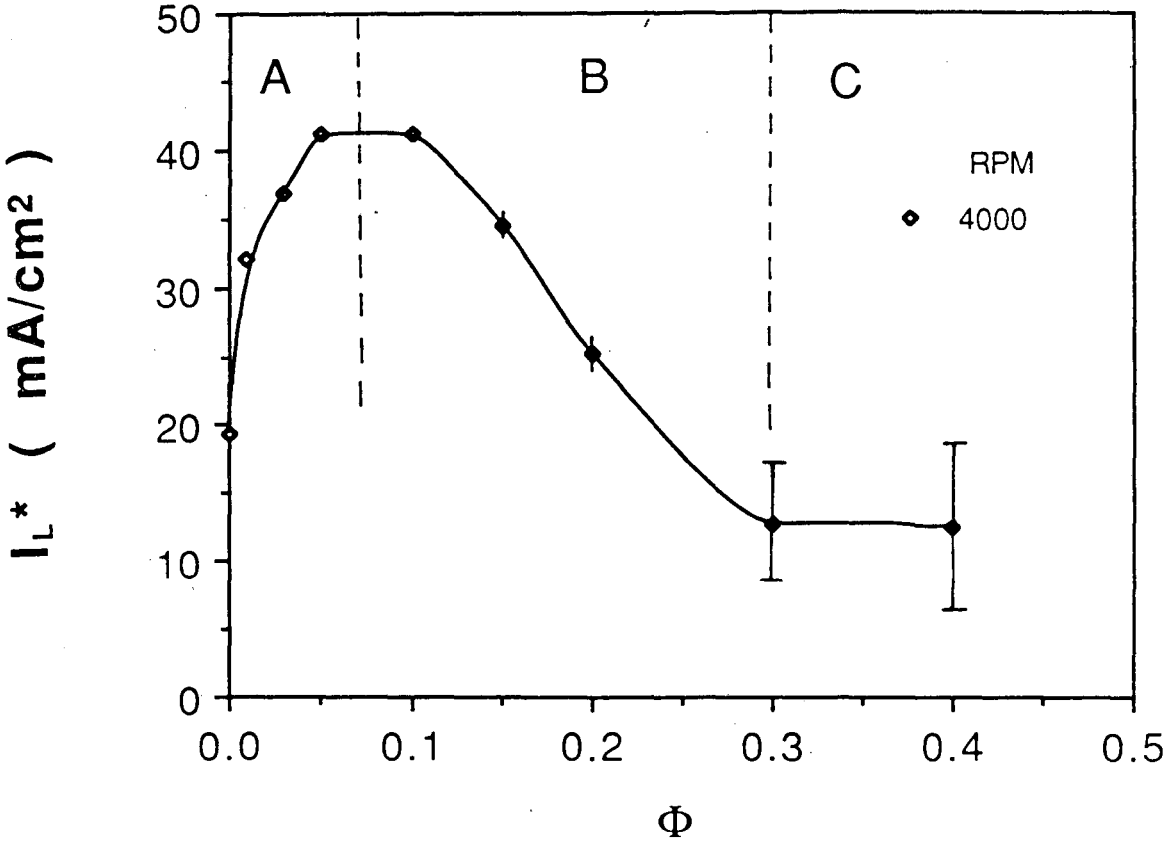

XBL 896-2425

Figure 7

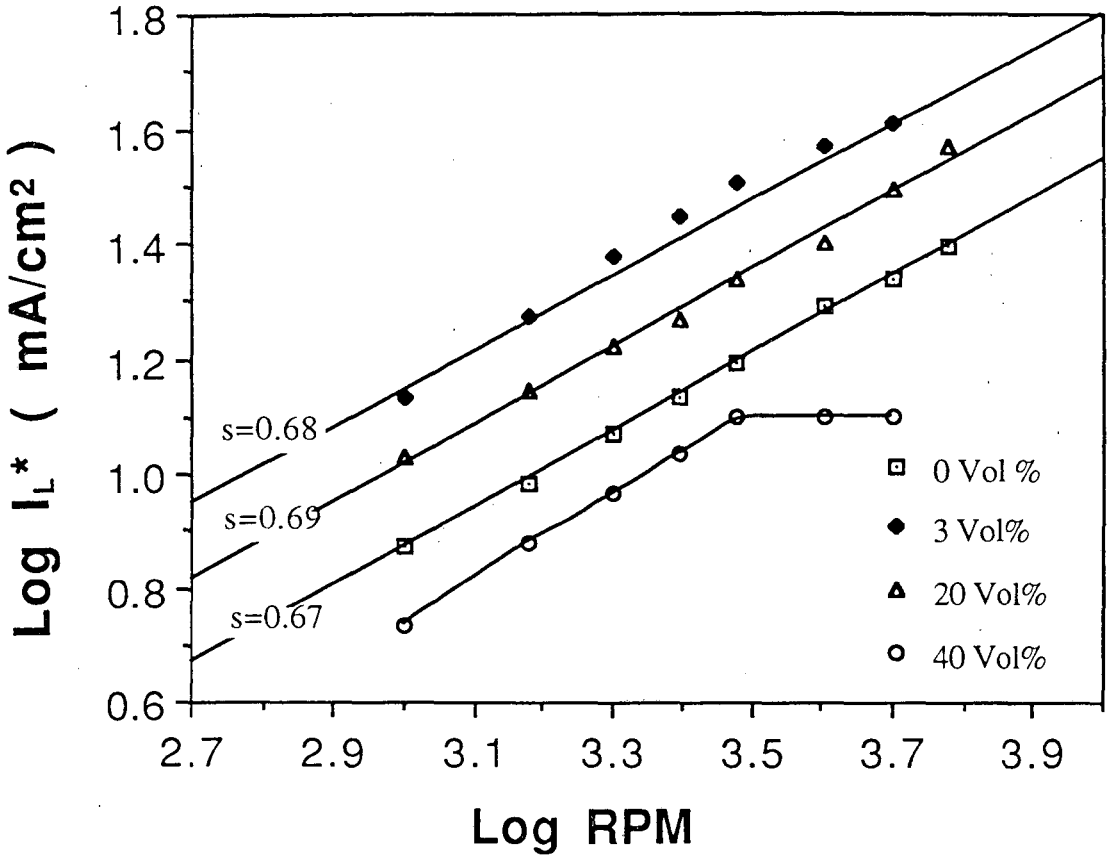

XBL 896-2426

Figure 8

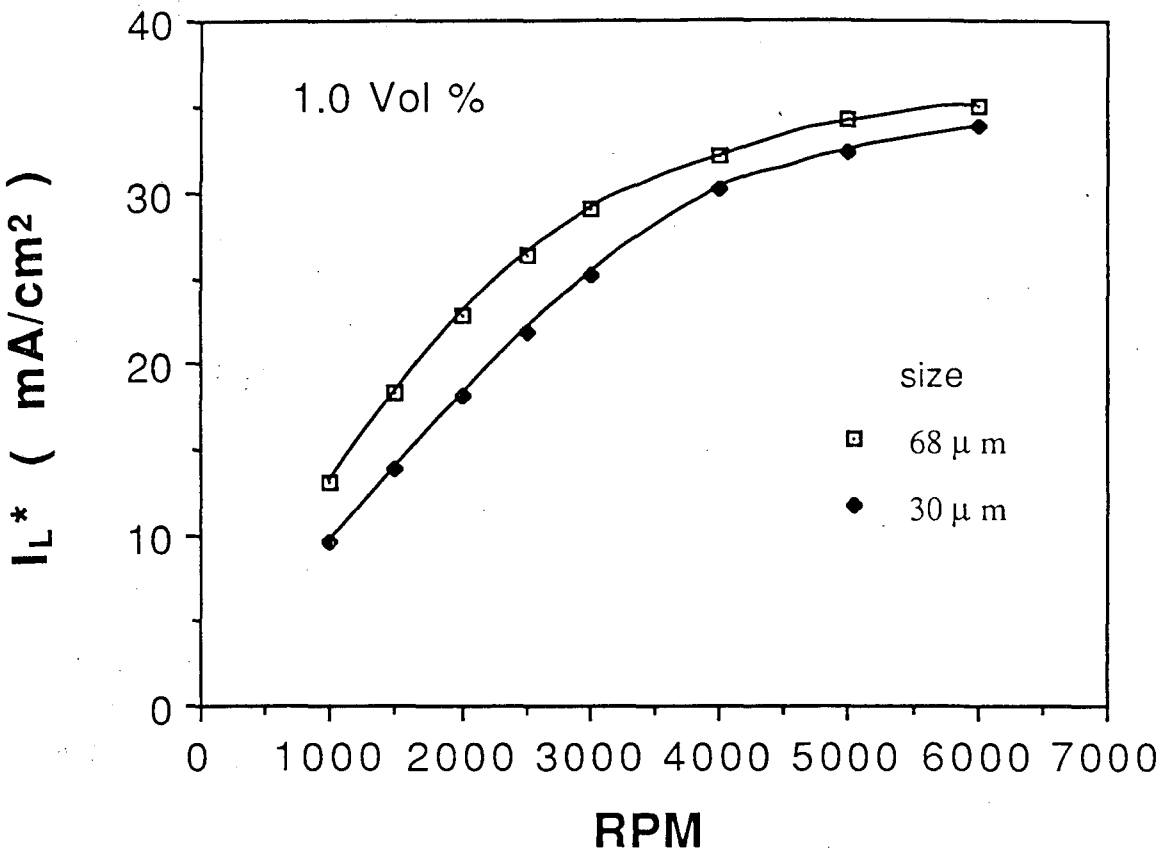

XBL 896-2427

Figure 9

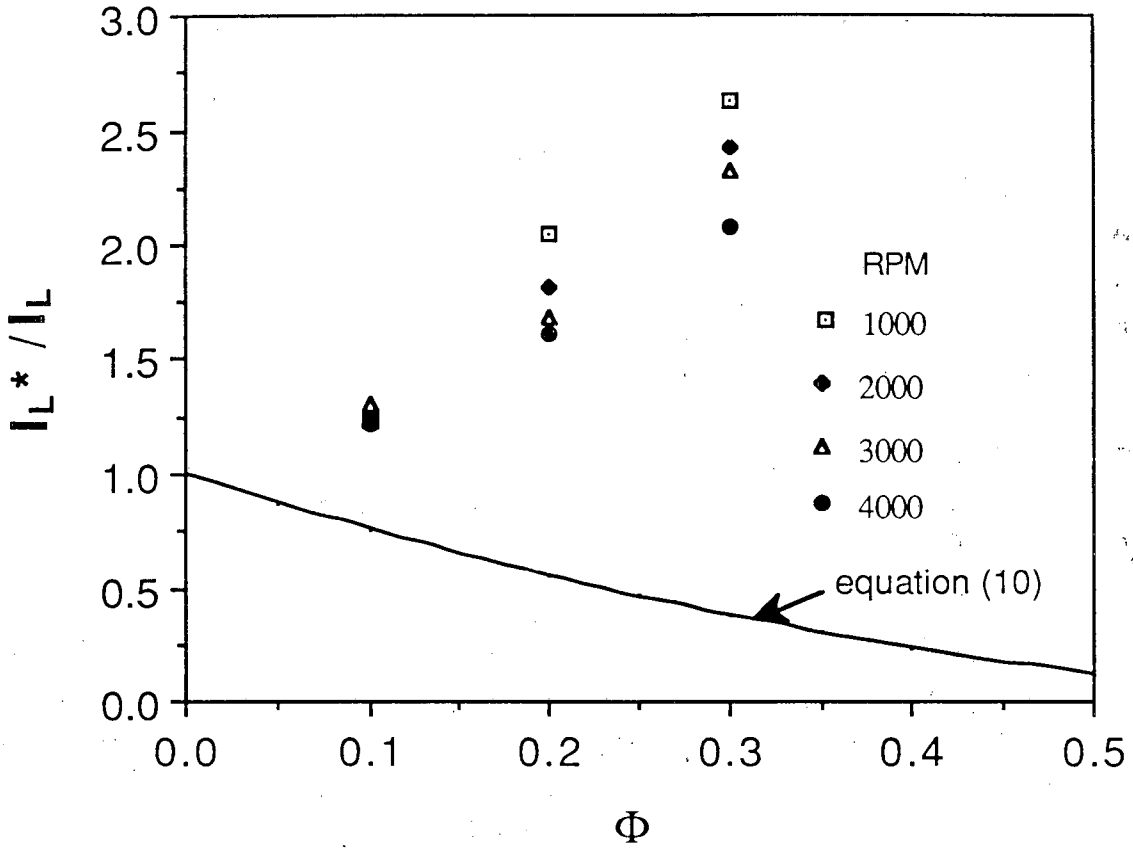

XBL 896-2428

Figure 10

LAWRENCE BERKELEY LABORATORY
TECHNICAL INFORMATION DEPARTMENT
1 CYCLOTRON ROAD
BERKELEY, CALIFORNIA 94720